Journal of Hazardous Materials Letters 6 (2025) 100158

Contents lists available at ScienceDirect

Journal of Hazardous Materials Letters

journal homepage: www.sciencedirect.com/journal/journal-of-hazardous-materials-letters

Development of a fluorophilic ion-exchange material with dual binding mechanism for solid-phase extraction of PFAS

Johanna Freilinger [a], Jan O. Back [b], Raphael Plangger [c], Herwig Schottenberger [a], Christian W. Huck [a], Marco Rupprich [c,d,*], Rania Bakry [a,1]

[a] Institute of Analytical Chemistry and Radiochemistry, Leopold-Franzens-University Innsbruck, Austria
[b] Department of Environmental, Process & Energy Engineering, MCI – The Entrepreneurial School, Innsbruck, Austria
[c] ionOXess GmbH, Innsbruck, Austria
[d] Institute for Ecopreneurship, School of Life Sciences, University of Applied Sciences and Arts Northwestern Switzerland (FHNW), Switzerland

ARTICLE INFO

Keywords:
PFAS
Solid-phase extraction
Fluorophilic polymer
Adsorption
Environmental analysis
Ion exchange

ABSTRACT

Per- and polyfluoroalkyl substances (PFAS) are persistent contaminants for which authorities worldwide have imposed limits on drinking water, groundwater and surface water. This has created challenges in PFAS detection, leading to an urgent need for reliable and selective solid-phase extraction (SPE) materials for PFAS analysis. In addressing this demand, we have tailored highly crosslinked copolymers containing 3-(1*H*,1*H*,2*H*,2*H*-perfluorooctyl)-1-vinylimidazolium chloride as a comonomer with ethylene dimethacrylate in various molar ratios. For ionic fluorosurfactants, these copolymers feature a dual binding mechanism that synergistically combines fluorophilic interactions and electrostatic attraction, enhancing selectivity and efficiency. The adsorption behavior of short- and long-chain PFAS and their recoveries were evaluated and compared to commercial SPE cartridges. Characterization revealed the highest ion-exchange capacity (412.7 ± 22 μeq g^{-1}) for a monomer-to-crosslinker ratio of 2:1. The dynamic adsorption capacities for various PFAS ranged from 15.2 to 306 g^{-1}. Recovery experiments consistently demonstrated high PFAS recoveries (98.8–121.6 %), while enrichment studies from wastewater confirmed its robustness in complex environmental matrices (recoveries: 90.8–99.2 %). Additionally, reusability experiments showed consistent recoveries over five cycles (recoveries: 90.34–108.0 %). The findings underscore the potential of this innovative polyelectrolyte as a selective, regenerable, and efficient alternative to conventional SPE materials, qualifying it as a superior candidate for PFAS analysis.

1. Introduction

Per- and polyfluoroalkyl substances (PFAS) are persistent environmental pollutants that have gained widespread public attention due to their considerable threats to human health and ecosystems (Brunn et al., 2023; Freilinger et al., 2025a; Glüge et al., 2020). Manufacturers and consumers transitioned to short- chain PFAS (< 7 carbon) in order to reduce the hazards associated with long-chain PFAS (Zhang et al., 2019). However, short-chain PFAS are equally persistent in water and soil, and exhibit higher aqueous solubility, associated with higher mobility and plume formation. Further, similar to long-chain PFAS (Li et al., 2020), severe health and ecotoxicological concerns have been attributed to such 'regrettable substitutes' (O'Rourke et al., 2024), meanwhile even including trifluoroacetate (Garavagno et al., 2024; Hanson et al., 2024). Concurrently, regulatory authorities worldwide have progressively diminished acceptable PFAS limits in drinking water, groundwater, and surface water (Cousins et al., 2022).

Due to the challenges associated with the trace quantification of PFAS in complex matrices such as surface water and groundwater, the development of sensitive and reliable analytical methods is of paramount importance (Jahnke and Berger, 2009; Mulabagal et al., 2018). Appropriate extractive sample preparation is required in order to concentrate the analytes of interest while removing the interfering matrix (Jia et al., 2022). Liquid-liquid extraction (LLE) and solid-phase extraction (SPE) are among the most widely applied methods for the extraction, purification and pre-concentration of PFAS, with the SPE

* Correspondence to: Institute for Ecopreneurship, School of Life Sciences, University of Applied Sciences and Arts Northwestern Switzerland (FHNW), Hofackerstrasse 30, Muttenz CH-4132, Switzerland.
E-mail address: marco.rupprich@fhnw.ch (M. Rupprich).
[1] Author passed away before the completion of this work.

https://doi.org/10.1016/j.hazl.2025.100158
Received 1 April 2025; Received in revised form 6 July 2025; Accepted 13 July 2025
Available online 13 July 2025

being used more commonly (Androulakakis et al., 2022; Groffen et al., 2019; Liu et al., 2020; Teymoorian et al., 2023). The most frequently used sorbents for PFAS are weak anion exchange mixed-mode sorbents as well as lipophilic-hydrophilic balance sorbents (Al Amin et al., 2020; Brumovský et al., 2018; Iannone et al., 2024; Wang et al., 2018). Ion exchangers (IEX) are usually resin beads made from neutral copolymers containing positively charged exchange sites giving PFAS the opportunity to bind to the hydrophobic backbone with the fluorocarbon tail, and, simultaneously, to the positively charged moiety of the resin with the negatively charged head of the fluorosurfactant, i.e. by a dual binding mode (Dixit et al., 2021; Woodard et al., 2017; Woodard et al., 2018). However, anion exchange resins also have a high affinity for inorganic anions that are abundant in natural and industrial water streams (Hu et al., 2016; Maimaiti et al., 2018). Consequently, the presence of ions and organic matter can interfere with the adsorption performance of PFAS, in particular at trace levels (Ateia et al., 2019; Butzlaff et al., 2025; Du et al., 2015; Rahman et al., 2014).

In order to achieve more PFAS-selective adsorption characteristics, research focus has shifted to the development of sorbents that incorporate fluorinated segments and provide specific F–F interaction (fluorophilicity) with the omniphobic fluoroponytail of PFAS (Singh et al., 2023; Tan et al., 2022b). Fluorosorbents that have been introduced include modified inorganic materials (Du et al., 2016; Medha et al., 2024; Singh et al., 2023; Wang et al., 2018), organic materials (Koda et al., 2015; Kumarasamy et al., 2020; Manning et al., 2022; Quan et al., 2020; Tan et al., 2022a), framework materials (Chen et al., 2015; He et al., 2022; Li et al., 2022), and molecularly imprinted polymers (Tasfaout et al., 2023). While fluorophilicity enables a targeted approach for PFAS capture, monofunctional fluorosorbents often suffer from low adsorption capacities and limited removal efficiency. Therefore, increasing attention has turned to multifunctional materials that combine fluorophilic interactions with additional binding modes.

In particular, the integration of ion exchange sites with fluorinated domains provides a complementary dual binding strategy, improving both affinity and selectivity for anionic PFAS (Fu et al., 2024; He et al., 2024a). This approach benefits from electrostatic attraction of the negatively charged PFAS headgroups and fluorophilic partitioning of the fluorinated tails, leading to synergistic retention. Singh et al. (2023) demonstrated the potential of this concept using a silica-based scaffold with closely positioned charged and fluorinated sites. However, the use of covalent siloxane bonds in these materials may compromise hydrolytic stability and may lead to leaching of cationic fluorosurfactants (Kaden et al., 2017), which could interfere with PFAS analysis by forming ion pairs. Similarly, materials developed by Chavan et al. (2018) show limitations such as low selectivity, non-switchable ionic character, and restricted reusability.

The present research introduces a polymer utilizing 3-(1*H*,1*H*,2*H*,2*H*-perfluorooctyl)-1-vinylimidazolium) chloride, [212684 4-17-3], a now commercially available monomer (Partl et al., 2021). Consequently, the polymer consists of repeating units that contain a cationic group with covalently attached fluorinated alkyl chains in close proximity. Therefore, this material presents a stable, regenerable polymer featuring a dual binding mechanism for selective enrichment of PFAS from aqueous matrices.

2. Materials and methods

2.1. Chemicals

The chemicals 1-propanol, 2,2-dimethoxy-2-phenylacetophenone (DMPA, 99 %), aluminium oxide (Al_2O_3, ca. 150 mesh), ammonium acetate (NH_4OAc, ≥ 97 %), ammonium chloride (NH_4Cl, z.A, ACS, ISO, PH.EUR.), ammonium hydroxide solution (NH_4OH, 25 % in water), ammonium perfluoro (2-methyl-3-oxahexanoate) (GenX, 95 %), acetonitrile (for LC-MS, ≥99.95 %), diclofenac sodium salt (98 %), ethylene dimethacrylate (EDMA, 98 %), formic acid (FA, 98–100 %), heptadecafluorooctanesulfonic acid potassium salt (PFOS, ≥ 92 %), lithium chloride (LiCl, ≥ 99 %), methanol (for LC-MS, hyper grade), perfluorobutanoic acid (PFBA, analytical standard), perfluoro-n-($^{13}C_8$) octanoic acid (13PFOA, IS, > 99 %), perfluorooctanoic acid (PFOA, 96 %), sodium bicarbonate ($NaHCO_3$, ≥ 99.7 %), sodium carbonate anhydrous (Na_2CO_3, ≥ 99.5 %), sodium chloride (NaCl, Reag. Ph. Eur.), sodium iodide (NaI, anhydrous) were obtained from various suppliers (abcr, Apollo Scientific, Carl Roth, Honeywell, Manchester Organics, Merck, Sigma-Aldrich, Thermo Fisher Scientific, Th. Geyer, Wellington Laboratories). For analysis, purified water from a Merck Millipore Milli-Q™ Reference Ultrapure Water Purification System with deionized water was used.

2.2. Polymer synthesis

For polymer preparation, 400 mg of the F-monomer, CAS RN 2126844-17-3, (Partl et al., 2021) and varied amounts of the crosslinker (EDMA) were combined with 200 mg H_2O, 500 mg ACN, and 500 mg 1-propanol functioning as porogens (Fig. 1). 40 mg DMPA were used as initiator for polymerization. To determine the optimum composition, the mass ratio of F-monomer to crosslinker was varied as 1:1, 2:1, 3:1, and 4:1.

The solution was sonicated for five minutes and then inserted between two glass plates. The polymerization with UV light was performed by exposing the mixture to an UV lamp operating at 8 W and 254 nm (CX-2000 UV Crosslinker, UVP Upland) for 30 min. The polymer was dried overnight at 65 °C. It was ground and sieved (AS 200 basic, Retsch) to obtain particles between 50 µm and 500 µm. The polymer was washed through a funnel filter (DURAN®, porosity 3) with water, ACN, MeOH, and dried again at 65 °C.

2.3. Physiochemical characterization

The obtained F-polymers were characterized via scanning electron microscopy, attenuated total reflectance (ATR) Fourier-transform infrared (FTIR) spectroscopy, physisorption of N_2 at 77 K, and thermogravimetric analysis (TGA). The details of each method are described in the Supplementary material.

2.4. Ion chromatography and PFAS analysis

Ion chromatography using a Dionex IC-2500 system and PFAS analysis using HPLC-MS/MS are described in the Supplementary material.

2.5. Solid-phase extraction (SPE)

2.5.1. Preparation of SPE cartridges

SPE cartridges were prepared by packing 25 mg polymer in an empty cartridge (1 cc, PP, with 20 µm PE frits, Merck). Dynamic adsorption and recovery experiments were also performed with Waters Oasis® WAX (weak anion exchange) 1 cc cartridges filled with 30 mg sorbent material as reference. The detailed workflow is described in the Supplementary material.

2.5.2. Ion-exchange capacity

The packed SPE cartridges were conditioned with 3 mL of a 0.1 M NaCl solution at a speed of 1 drop per 2 s by using pressurized air at

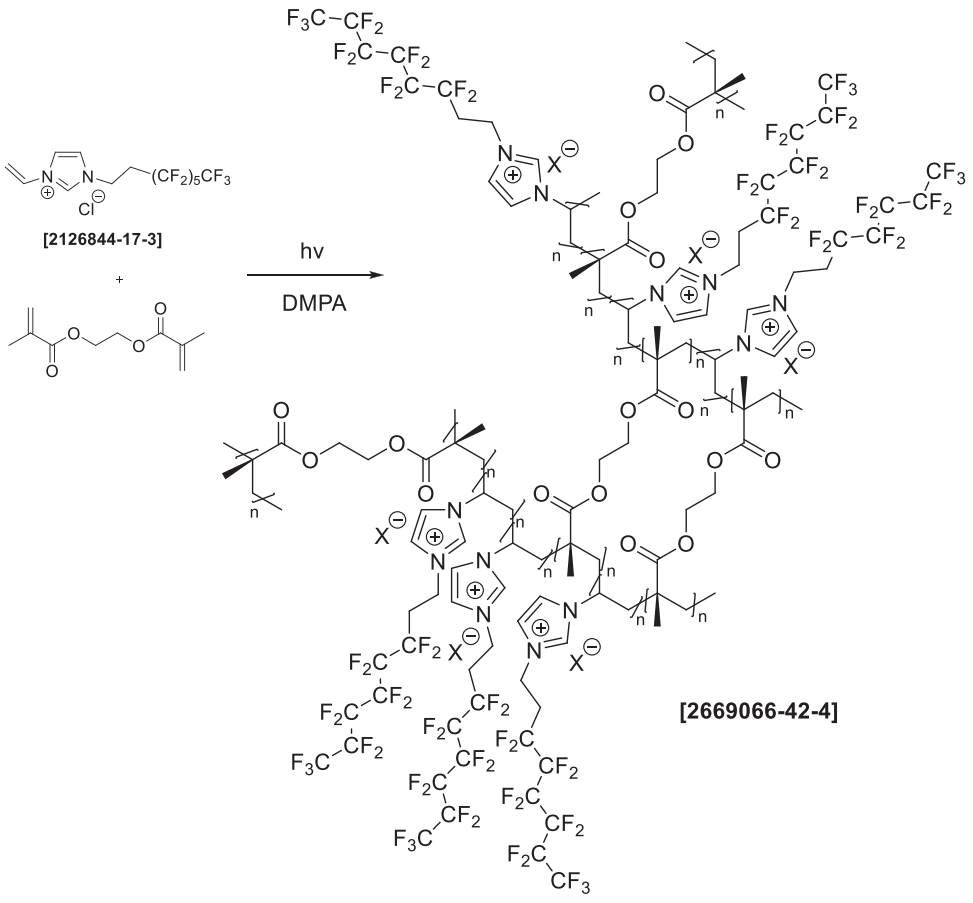

Fig. 1. Synthesis of the F-polymer with perfluorohexyl-ethyl-tethered polyvinylimidazolium chloride crosslinked by EDMA.

1 bar. Afterwards, the material was washed with 6 mL of water. The last mL was collected for control measurements. 3 mL of a 0.1 M NaI solution were then added to substitute the original chloride of the IEX resin. The eluate was collected and diluted to 10 mL before measurements with ion chromatography to determine the chloride content. The polymer with the F-monomer-to-crosslinker ratio showing the highest ion-exchange capacity (IEC) was selected for further experiments.

2.5.3. Dynamic adsorption capacity

SPE cartridges packed with the optimized polymer (ratio vinylimidazolium Cl^- to EDMA 2:1 w/w) were conditioned with 1 mL MeOH and 1 mL water and then loaded with 1 mL PFOA (1000 mg L^{-1}) solutions. The eluate concentration was measured until a plateau was reached, so that a specific-throughput breakthrough curve could be obtained. The experiment was repeated with GenX (polymer: 100 mg L^{-1}, WAX: 400 mg L^{-1}). Furthermore, the selectivity towards PFAS was assessed by measuring the dynamic adsorption capacity with a mixture of NaCl, diclofenac, and GenX (polymer: 60 mg L^{-1}, WAX: 40 mg L^{-1}) using a ratio of 4:2:1 (w/w/w). The Thomas model (Thomas, 1944) was fitted to the experimental breakthrough data using Eq. (1), from which the dynamic adsorption capacity q_0 was calculated.

$$\ln\left(\frac{C_0}{C_t}-1\right)=\frac{k_{Th}}{Q}q_0 m-\frac{k_{Th}}{Q}C_0 V \quad (1)$$

2.5.4. Recovery and enrichment experiments

To determine the recovery of the materials, the optimized polymer as well as Oasis® WAX were loaded with a standard containing 100 µg L^{-1} of each, PFBA, GenX, PFOA, and PFOS (1 mL), followed by elution. Recoveries were calculated based on the PFAS mass quantified in the eluate, representing the total amount recovered from the sorbent under the given conditions. Additionally, enrichment experiments were carried out in spiked wastewater (0.5 µg L^{-1} of each PFAS) to determine the effect of complex water matrices on the recovery of the optimized polymer. Consequently, both low (environmental) and high (laboratory) PFAS concentration ranges are encompassed within the experimental framework.

2.5.5. Cyclic stability

The reusability of the material was evaluated through cyclic adsorption/desorption studies. One cycle involved loading SPE cartridges packed with either F-polymer or Oasis® WAX with 100 µg L^{-1} PFAS solutions, followed by elution. The material was dried with pressurized air for 5 min before reloading.

2.5.6. pH effects

In order to detect potential hydrolysis of the F-polymer under acidic or alkaline conditions, the material was conditioned at pH 2 and 11 prior to PFAS adsorption. Additionally, the effect of the pH on adsorption was examined by adjusting the pH of the PFAS solution to 4 and 10. Details are described in the Supplementary materials.

3. Results and discussion

3.1. F-monomer-to-crosslinker ratio

The surface morphology of the synthesized F-polymers is illustrated by the SEM images, which reveal differences in porosity based on varying F-monomer-to-crosslinker ratios (Fig. 2a–d). A comparison of these images reveals that polymers produced with 1:1 and 2:1 ratios have a significantly more open-porous morphology than those synthesized with 3:1 and 4:1 ratios. Furthermore, the surface features observed

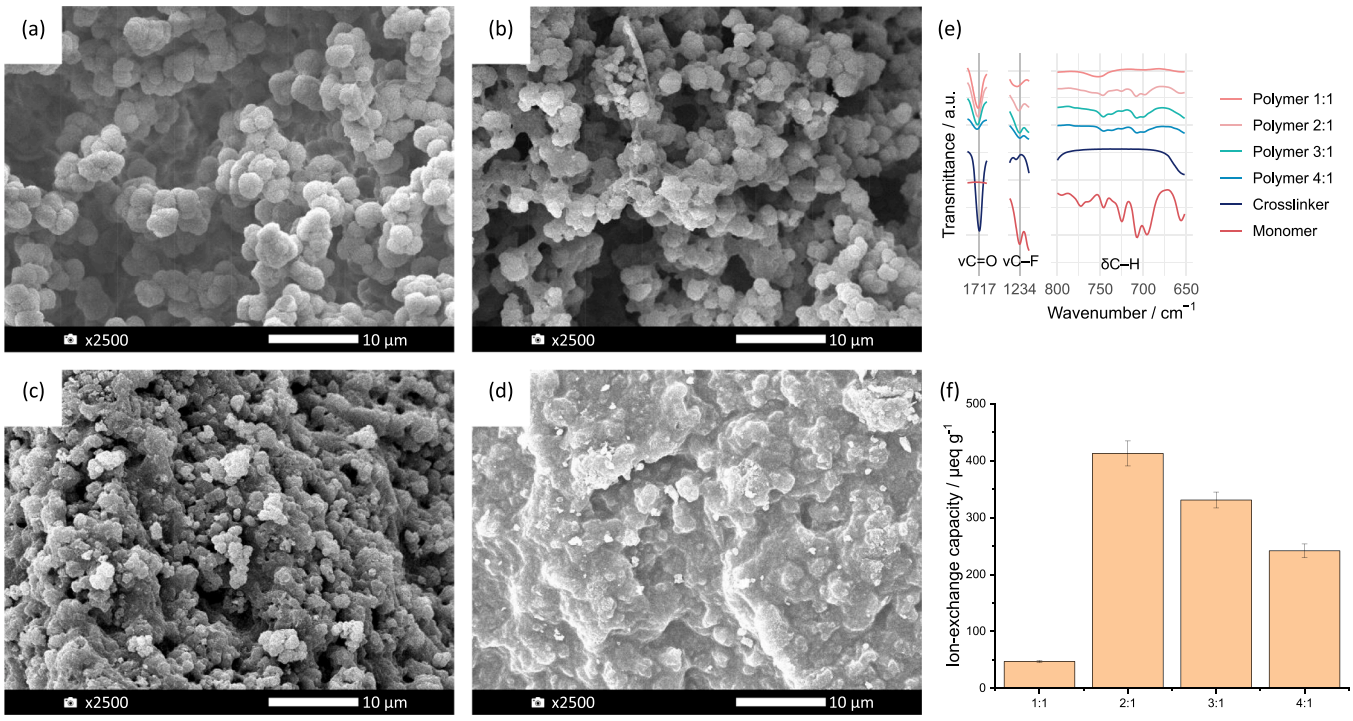

Fig. 2. Scanning electron micrographs of polymers with F-monomer-to-crosslinker ratio 1:1 (a), 2:1 (b), 3:1 (c) and 4:1 (d) at a magnification of 2500x, bar represents 10 µm. (e) Fourier-transform infrared spectra in transmission of F-monomer, crosslinker and the synthesized polymers. (f) Ion-exchange capacity (IEC) of the synthesized polymers (means, standard deviations, $n = 3$).

in the SEM images are indicative of higher adsorption capacities in polymers 1:1 and 2:1 in comparison to polymers 3:1 and 4:1, thus qualifying them more appropriate for utilization in PFAS adsorption applications. Physisorption analysis (Fig. S2a,b) confirmed higher porosities at lower F-monomer-to-crosslinker ratios. Furthermore, TGA (Fig. S2c,d) demonstrated thermal stability up to approx. 200 °C, beyond which thermal decomposition took place in accordance with the imidazolium group (Singh et al., 2023).

Analysis of the FTIR spectra (Fig. 2e, Fig. S2e) reveals characteristic absorption regions corresponding to both the imidazolium derivative and crosslinker, which are also present in the synthesized polymers. Notably, a distinct absorption band at 1717 cm^{-1}, attributed to the C═O stretching vibration of the crosslinker, is observed, whereas the heterocyclic constituent does of course not exhibit a band in this region. A comparative evaluation of this peak across the polymer samples indicates a progressive increase in transmission with increasing imidazolium content. Conversely, the spectral region between 630 and 800 cm^{-1} displays characteristic bands associated with the cationic F-monomer, primarily corresponding to specific C–H deformation vibrations, while the crosslinker does not contribute significantly to this range. Additionally, an absorption band at 1234 cm^{-1}, indicative of C–F stretching vibrations, further confirms the presence of the fluoroponytailed moieties. These findings suggest that all four polymer samples incorporate both, cationic fluorosurfactant and crosslinker in varying proportions.

The IEC is indicative of the binding potential of negatively charged ions, and thus suitable for a preliminary assessment of PFAS acid adsorption capacities. The IEC of the polymer synthesized with a 2:1 imidazolium-to-crosslinker ratio is the highest, reaching 412.7 ± 22 µeq g^{-1} (Fig. 2f). This supports the observation from SEM and physisorption experiments, according to which copolymers with ratios of 3:1 (330.9 ± 14 µeq g^{-1}) and 4:1 (241.7 ± 12 µeq g^{-1}) exhibit insufficient porosity to facilitate efficient ion exchange, while the 1:1 ratio demonstrates a significantly lower capacity of 47.03 ± 1.9 µeq g^{-1}. Whilst common commercial ion-exchange materials demonstrate IECs of approx. 1 meq g^{-1} (Dixit et al., 2021), for SPE applications, PFAS specificity is the most significant factor (Androulakakis et al., 2022). Based on these results, a F-monomer salt-to-crosslinker ratio of 2:1 (w/w) was selected for further experimental investigations.

3.2. Dynamic adsorption capacity

The dynamic adsorption capacities obtained from the synthesized polymer with a imidazolium-to-crosslinker ratio of 2:1 were compared to commercially available Oasis® WAX cartridges (Fig. 3a–c). A distinct trend can be observed when comparing the fluoroalkyl-tethered copolymer to the WAX cartridges. According to the Thomas model, under aqueous standard conditions, the WAX material exhibits superior adsorption capacities for PFOA (504 mg g^{-1}) and GenX (84.3 mg g^{-1}) compared to the optimized polymer, which achieves 306 mg g^{-1} for PFOA and 33.3 mg g^{-1} for GenX (Table S2). In comparison, the median PFOS isotherm uptake capacities of different ion-exchange resins are reported to be approx. 400 µeq g^{-1} (i.e., 200 mg g^{-1}) (Dixit et al., 2021). However, it should be noted that the experimental conditions (resin dosage, PFAS concentrations, and water matrix) reported in literature vary widely and influence the measured capacity significantly.

However, when competing anions such as diclofenac and Cl$^-$ are introduced, both of which compete with PFAS for binding sites, the newly evaluated polymer outperforms the WAX cartridges. Specifically, the GenX capacity of the polymer decreases by 54 % to 15.2 mg g^{-1}, whereas the WAX material exhibits a more pronounced decline of 86 %, reducing its capacity to 11.8 mg g^{-1}. These findings support the hypothesis that, expectedly, fluorine-fluorine (F–F) interactions contribute to a more selective PFAS-binding to the polymer, in contrast to common ion exchange materials, where adsorption is primarily governed by electrostatic interactions. Furthermore, in contrast to the fluorous polymer, the WAX material does not exhibit a well-defined breakthrough curve in the presence of competing ions, making it challenging to determine the exact point at which PFAS adsorption ceases—a further indication that more accurate analytical methods may be possible by

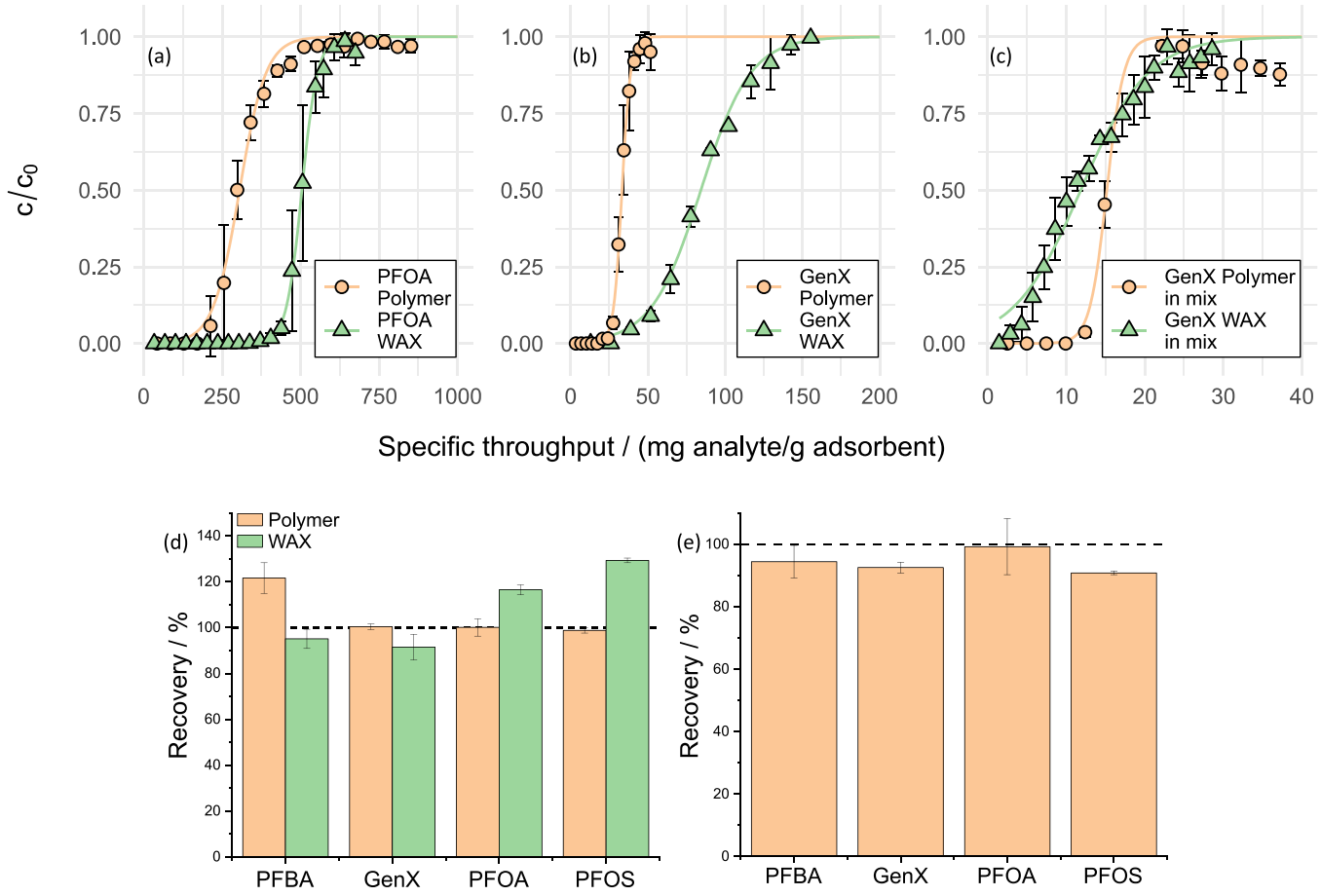

Fig. 3. Breakthrough curves (means, standard deviations, $n = 3$) and recoveries of F-polymer 2:1 and WAX. (a) Breakthrough with PFOA. (b) Breakthrough with GenX. (c) Breakthrough with a mixture of GenX:diclofenac:NaCl (1:2:4). (d) Recoveries of PFBA, GenX, PFOA, and PFOS. (e) Recoveries after PFAS enrichment from spiked effluent wastewater.

taking advantage of supportive fluorophilic interactions.

The proposed binding mechanism (Fig. S1) is substantiated by theoretical insights into F–F interactions (Fu et al., 2024), evidence from shifts in the ^{19}F NMR peaks (He et al., 2024b; Koda et al., 2014), and previous studies employing positively charged moieties and fluorine chains on a silicon-based backbone (Singh et al., 2023). The potential for computational studies to provide further insight into the interaction of PFAS and polymers has been recently confirmed through the utilization of a global optimization (MACE-OFF23) neural network potential approach (Freilinger et al., 2025b).

3.3. Recovery, reusability, and pH effects

The recoveries of PFBA, GenX, PFOA, and PFOS were tested for both, the synthesized F-polymer 2:1 and the commercially available Oasis® WAX cartridges (Fig. 3d). The results indicate consistently high recoveries for all four PFAS across both materials. The fluoroalkyl-tethered copolymer exhibited recoveries ranging from 98.8 % (PFOS) to 121.6 % (PFBA), with relative standard deviation (RSD) values below 6 %. Similarly, the Oasis® WAX material demonstrated recoveries between 95.05 % (PFBA) and 129.2 % (PFOS) and RSD values lower 6.5 %. These findings confirm that the F-polymer performs comparably to the WAX cartridges, demonstrating its suitability for SPE of both short-chain and long-chain PFAS.

Furthermore, the enrichment of PFAS from spiked effluent wastewater samples was measured using F-polymer 2:1 and the recoveries were calculated (Fig. 3e). The synthesized material demonstrated recoveries ranging from 90.8 % for PFOS to 99.2 % for PFOA, with RSD values below 10 %. These findings suggest that the F-polymer is well-suited for the enrichment of PFAS from complex water matrices containing dissolved organic matter, electrolytes, and further components that potentially diminish the binding affinity of PFAS.

Additionally, the reusability of both materials over multiple cycles was investigated. The F-polymer maintained consistently high recoveries across all five cycles (90.34–108.0 %), whereas the WAX cartridge exhibited a decline in performance, with recoveries dropping from 91.29–122.9 % to 34.60–51.12 % after only two cycles (Fig. 4).

Moreover, the pH stability of both materials was assessed. Neither conditioning at pH 2 or 11 nor loading with a PFAS solution at pH 4 affected adsorption performance. Only in the case of WAX cartridges did the uptake of PFBA decrease to 90 % when the PFAS solution was adjusted to pH 10 (Fig. S5).

4. Conclusion

In the context of escalating regulatory restrictions on perfluoroalkyl substances (PFAS), we have tailored organic ion exchange materials for the selective and reliable detection of PFAS acids by solid phase extraction (SPE). These highly crosslinked copolymers are readily accessible from commercial precursors, containing 3-(1*H*,1*H*,2*H*,2*H*-perfluorooctyl)-1-vinylimidazolium chloride as a comonomer with ethylene dimethacrylate. For ionic fluorosurfactants, they feature a dual binding mechanism that synergistically combines fluorophilic interactions and electrostatic attraction, thus enhancing selectivity and binding efficiency.

The synthesized F-polymer demonstrated a well-defined porous

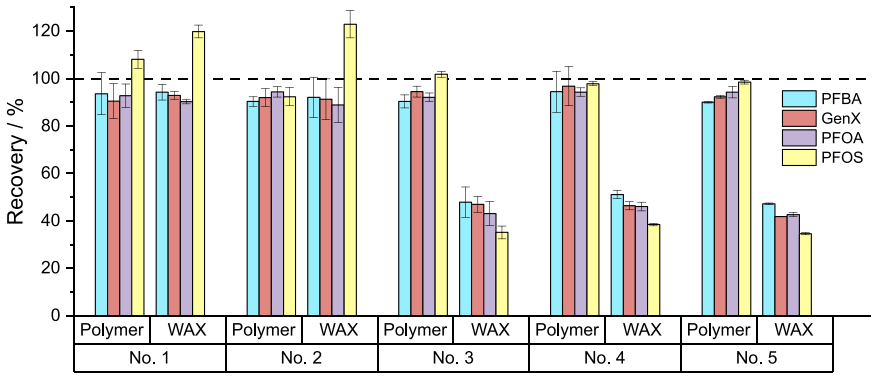

Fig. 4. Cyclic loading studies with PFBA, GenX, PFOA, and PFOS for the F-polymer 2:1 and WAX (means, standard deviations, $n = 3$).

morphology, with the 1:1 and 2:1 F-monomer-to-crosslinker ratios exhibiting the highest apparent porosity in scanning electron micrographs and physisorption studies, suggesting enhanced adsorption capacities. ATR-FTIR analysis confirmed the incorporation of both F-monomer and crosslinker in all F-polymer samples. Ion-exchange capacity measurements revealed that the 2:1 ratio exhibited the highest capacity (412.7 ± 22 μeq g^{-1}), leading to its selection for further studies. Dynamic adsorption experiments indicated that, under standard aqueous conditions, the F-polymer displayed lower adsorption capacities for PFOA and GenX compared to the commercial Oasis® WAX material. However, in the presence of competing organic and inorganic anions, it outperformed the WAX cartridges, highlighting the role of fluorine-fluorine (F–F) interactions in selective PFAS binding, which is attributed to the F-monomer. This specificity is particularly advantageous in complex environmental matrices, where non-target anions may otherwise interfere with adsorption.

Additionally, recovery experiments demonstrated that the F-polymer performed comparably to the WAX cartridges, with high recoveries (98.8–121.6 %) and low RSD values (<6 %) for PFBA, GenX, PFOA, and PFOS. Furthermore, enrichment studies in effluent wastewater confirmed its effectiveness in complex matrices, with recoveries ranging from 90.8 % to 99.2 % and RSD values below 10 %. The reusability of both materials revealed that the F-polymer maintained consistently high recoveries over five cycles (90.34–108.0 %), while the WAX cartridge showed a decline from 91.29–122.9 % to 34.60–51.12 % after just three cycles. In order to establish the hydrolytic stability, the F-polymer was subjected to varying pH conditions, without any reduction in PFAS uptake; however, additional long-term studies are recommended to confirm this finding.

Overall, these findings demonstrate that the F-polymer newly introduced as SPE sorbent is a viable alternative to commercially available WAX materials for PFAS extraction, particularly in samples containing competing anions. Its high selectivity and strong performance in complex water matrices make it a promising candidate for environmental PFAS analysis and remediation applications. In order to verify the proposed dual binding mechanism, clarify the respective contributions of electrostatic and fluorophilic partitioning, and to assist in future material optimization, further experimental and computational approaches are required. Furthermore, long-term stability should be assessed through extended adsorption/desorption cycling under varying pH and water matrix conditions, complemented by post-use structural characterization (e.g., SEM or TGA) to evaluate material integrity.

CRediT authorship contribution statement

Rania Bakry: Supervision, Funding acquisition, Conceptualization. **Johanna Freilinger:** Writing – original draft, Methodology, Investigation. **Raphael Plangger:** Methodology. **Back Jan O:** Writing – review & editing, Investigation, Funding acquisition. **Huck Christian W:** Resources. **Herwig Schottenberger:** Writing – review & editing, Conceptualization. **Marco Rupprich:** Writing – review & editing, Project administration, Funding acquisition.

Funding information

This work is part of a project PFAS-Trap (Project no. C220002), funded by the Federal Ministry Republic of Austria, Climate Action, Environment, Energy, Mobility, Innovation and Technology.

Supplementary Material

Link to be provided by Journal.

Declaration of Competing Interest

The authors declare that they have no known competing financial interests or personal relationships that could have appeared to influence the work reported in this paper.

Acknowledgements

This work is part of a project PFAS-Trap (Project no. C220002), funded by the Federal Ministry Republic of Austria, Climate Action, Environment, Energy, Mobility, Innovation and Technology. The assistance provided by Michael Kresta in TGA measurements is gratefully acknowledged.

Appendix A. Supporting information

Supplementary data associated with this article can be found in the online version at doi:10.1016/j.hazl.2025.100158.

Data availability

Data will be made available on request.

References

Al Amin, M., Sobhani, Z., Liu, Y., Dharmaraja, R., Chadalavada, S., Naidu, R., et al., 2020. Recent advances in the analysis of per-and polyfluoroalkyl substances (PFAS)—A review. Environ. technol. innov. 19, 100879. https://doi.org/10.1016/j.eti.2020.100879.

Androulakakis, A., Alygizakis, N., Bizani, E., Thomaidis, N.S., 2022. Current progress in the environmental analysis of poly- and perfluoroalkyl substances (PFAS). Environ. Sci.: Adv. 1 (5), 705–724. https://doi.org/10.1039/D2VA00147K.

Ateia, M., Alsbaiee, A., Karanfil, T., Dichtel, W., 2019. Efficient PFAS removal by amine-functionalized sorbents: critical review of the current literature. Environ. Sci. Technol. Lett. 6 (12), 688–695. https://doi.org/10.1021/acs.estlett.9b00659.

Brumovský, M., Bečanová, J., Karásková, P., Nizzetto, L., 2018. Retention performance of three widely used SPE sorbents for the extraction of perfluoroalkyl substances from seawater. Chemosphere 193, 259–269. https://doi.org/10.1016/j.chemosphere.2017.10.174.

Brunn, H., Arnold, G., Körner, W., Rippen, G., Steinhäuser, K.G., Valentin, I., 2023. PFAS: forever chemicals—persistent, bioaccumulative and mobile. Reviewing the status and the need for their phase out and remediation of contaminated sites. Environ. Sci. Eur. 35 (1), 1–50. https://doi.org/10.1186/s12302-023-00721-8.

Butzlaff, A.H., Mezgebe, B., Collins, A., Lin, Z.-W., Lassalle-Vega, D., Harmody, I.M., et al., 2025. Comparative evaluation of PFAS-selective adsorbents in hard-to-treat residual waste streams. Chem. Eng. J. 511, 161983. https://doi.org/10.1016/j.cej.2025.161983.

Chavan, S.N., Padhan, A.K., Mandal, D., 2018. Self-assembly of fluorous amphiphilic copolymers with ionogels and surface switchable wettability. Polym. Chem. 9 (17), 2258–2270. https://doi.org/10.1039/C8PY00273H.

Chen, T.-H., Popov, I., Kaveevivitchai, W., Chuang, Y.-C., Chen, Y.-S., Jacobson, A.J., et al., 2015. Mesoporous fluorinated metal–organic frameworks with exceptional adsorption of fluorocarbons and CFCs. Angew. Chem. 127 (47), 14108–14112. https://doi.org/10.1002/ange.201505149.

Cousins, I.T., Johansson, J.H., Salter, M.E., Sha, B., Scheringer, M., 2022. Outside the safe operating space of a new planetary boundary for per- and polyfluoroalkyl substances (PFAS). Environ. Sci. Technol. 56 (16), 11172–11179. https://doi.org/10.1021/acs.est.2c02765.

Dixit, F., Dutta, R., Barbeau, B., Berube, P., Mohseni, M., 2021. PFAS removal by ion exchange resins: a review. Chemosphere 272, 129777. https://doi.org/10.1016/j.chemosphere.2021.129777.

Du, Z., Deng, S., Chen, Y., Wang, B., Huang, J., Wang, Y., et al., 2015. Removal of perfluorinated carboxylates from washing wastewater of perfluorooctanesulfonyl fluoride using activated carbons and resins. J. Hazard. Mater. 286, 136–143. https://doi.org/10.1016/j.jhazmat.2014.12.037.

Du, Z., Deng, S., Zhang, S., Wang, B., Huang, J., Wang, Y., et al., 2016. Selective and high sorption of perfluorooctanesulfonate and perfluorooctanoate by fluorinated alkyl chain modified montmorillonite. J. Phys. Chem. C 120 (30), 16782–16790. https://doi.org/10.1021/acs.jpcc.6b04757.

Freilinger, J., Gelbrich, T., Braun, D.E., Griesser, U.J., Bakry, R., Kahlenberg, V., et al., 2025a. Ammonium 6: 2 fluorotelomer sulfonate: crystal structure, thermal analysis and use as internal standard in PFAS analysis. J. Mol. Struct. 1327, 141232. https://doi.org/10.1016/j.molstruc.2024.141232.

Freilinger, J., Kappacher, C., Huter, K., Hofer, T.S., Back, J.O., Huck, C.W., et al., 2025b. Interactions between perfluorinated alkyl substances (PFAS) and microplastics (MPs): findings from an extensive investigation. J. Hazard. Mater. Adv. 18, 100740. https://doi.org/10.1016/j.hazadv.2025.100740.

Fu, K., Huang, J., Luo, F., Fang, Z., Yu, D., Zhang, X., et al., 2024. Understanding the selective removal of perfluoroalkyl and polyfluoroalkyl substances via fluorine–fluorine interactions: a critical review. Environ. Sci. Technol. https://doi.org/10.1021/acs.est.4c06519.

Garavagno, Maria de los Angeles, Holland, R., Khan, M.A.H., Orr-Ewing, A.J., Shallcross, D.E., 2024. Trifluoroacetic acid: toxicity, sources, sinks and future prospects. Sustainability 16 (6), 2382. https://doi.org/10.3390/su16062382.

Glüge, J., Scheringer, M., Cousins, I.T., DeWitt, J.C., Goldenman, G., Herzke, D., et al., 2020. An overview of the uses of per-and polyfluoroalkyl substances (PFAS). Environ. Sci.: Process. Impacts 22 (12), 2345–2373. https://doi.org/10.1039/D0EM00291G.

Groffen, T., Lasters, R., Lemière, F., Willems, T., Eens, M., Bervoets, L., et al., 2019. Development and validation of an extraction method for the analysis of perfluoroalkyl substances (PFASs) in environmental and biotic matrices. J. Chromatogr. B 1116, 30–37. https://doi.org/10.1016/j.jchromb.2019.03.034.

Hanson, M.L., Madronich, S., Solomon, K., Sulbaek Andersen, M.P., Wallington, T.J., 2024. Trifluoroacetic acid in the environment: consensus, gaps, and next steps. Environ. Toxicol. Chem. 43 (10), 2091–2093. https://doi.org/10.1002/etc.5963.

He, C., Yang, Y., Hou, Y.-J., Luan, T., Deng, J., 2022. Chitosan-coated fluoro-functionalized covalent organic framework as adsorbent for efficient removal of per-and polyfluoroalkyl substances from water. Sep. Purif. Technol. 294, 121195. https://doi.org/10.1016/j.seppur.2022.121195.

He, Y., Cheng, X., Gunjal, S.J., Zhang, C., 2024a. Advancing PFAS sorbent design: mechanisms, challenges, and perspectives. ACS Mater. Au 4 (2), 108–114. https://doi.org/10.1021/acsmaterialsau.3c00066.

He, Y., Zhou, J., Li, Y., Yang, Y.-D., Sessler, J.L., Chi, X., 2024b. Fluorinated nonporous adaptive cages for the efficient removal of perfluorooctanoic acid from aqueous source phases. J. Am. Chem. Soc. 146 (9), 6225–6230. https://doi.org/10.1021/jacs.3c14213.

Hu, Y., Foster, J., Boyer, T.H., 2016. Selectivity of bicarbonate-form anion exchange for drinking water contaminants: influence of resin properties. Sep. Purif. Technol. 163, 128–139. https://doi.org/10.1016/j.seppur.2016.02.030.

Iannone, A., Carriera, F., Di Fiore, C., Avino, P., 2024. Poly-and Perfluoroalkyl Substance (PFAS) Analysis in Environmental Matrices: An Overview of the Extraction and Chromatographic Detection Methods. Analytica 5 (2), 187–202. https://doi.org/10.3390/analytica5020012.

Jahnke, A., Berger, U., 2009. Trace analysis of per-and polyfluorinated alkyl substances in various matrices—how do current methods perform? J. Chromatogr. A 1216 (3), 410–421. https://doi.org/10.1016/j.chroma.2008.08.098.

Jia, S., Marques Dos Santos, M., Li, C., Snyder, S.A., 2022. Recent advances in mass spectrometry analytical techniques for per- and polyfluoroalkyl substances (PFAS). Anal. Bioanal. Chem. 414 (9), 2795–2807. https://doi.org/10.1007/s00216-022-03905-y.

Kaden, W.E., Pomp, S., Sterrer, M., Freund, H.-J., 2017. Insights into silica bilayer hydroxylation and dissolution. Top. Catal. 60 (6), 471–480. https://doi.org/10.1007/s11244-016-0715-7.

Koda, Y., Terashima, T., Sawamoto, M., 2014. Fluorous microgel star polymers: selective recognition and separation of polyfluorinated surfactants and compounds in water. J. Am. Chem. Soc. 136 (44), 15742–15748. https://doi.org/10.1021/ja508818j.

Koda, Y., Terashima, T., Takenaka, M., Sawamoto, M., 2015. Star polymer gels with fluorinated microgels via star–star coupling and cross-linking for water purification. ACS Macro Lett. 4 (4), 377–380. https://doi.org/10.1021/acsmacrolett.5b00127.

Kumarasamy, E., Manning, I.M., Collins, L.B., Coronell, O., Leibfarth, F.A., 2020. Ionic fluorogels for remediation of per-and polyfluorinated alkyl substances from water. ACS Cent. Sci. 6 (4), 487–492. https://doi.org/10.1021/acscentsci.9b01224.

Li, F., Duan, J., Tian, S., Ji, H., Zhu, Y., Wei, Z., et al., 2020. Short-chain per-and polyfluoroalkyl substances in aquatic systems: occurrence, impacts and treatment. Chem. Eng. J. 380, 122506. https://doi.org/10.1016/j.cej.2019.122506.

Li, R., Adarsh, N.N., Lu, H., Wriedt, M., 2022. Metal-organic frameworks as platforms for the removal of per-and polyfluoroalkyl substances from contaminated waters. Matter 5 (10), 3161–3193. https://doi.org/10.1016/j.matt.2022.07.028.

Liu, Y., Bao, J., Hu, X.-M., Lu, G.-L., Yu, W.-J., Meng, Z.-H., 2020. Optimization of extraction methods for the analysis of PFOA and PFOS in the salty matrices during the wastewater treatment. Microchem. J. 155, 104673. https://doi.org/10.1016/j.microc.2020.104673.

Maimaiti, A., Deng, S., Meng, P., Wang, W., Wang, B., Huang, J., et al., 2018. Competitive adsorption of perfluoroalkyl substances on anion exchange resins in simulated AFFF-impacted groundwater. Chem. Eng. J. 348, 494–502. https://doi.org/10.1016/j.cej.2018.05.006.

Manning, I.M., Guan Pin Chew, N., Macdonald, H.P., Miller, K.E., Strynar, M.J., Coronell, O., et al., 2022. Hydrolytically stable ionic fluorogels for high-performance remediation of per- and polyfluoroalkyl substances (PFAS) from natural water. Angew. Chem. (Int. Ed. Engl.) 61 (41), e202208150. https://doi.org/10.1002/anie.202208150.

Medha, S., Romisher, Z., van Bramer, S., Weyrich, J., Khan, S., Saha, D., 2024. Enhanced adsorption of perfluorooctanesulfonic acid (PFOS) in fluorine doped mesoporous carbon: experiment and simulation. Carbon 218, 118745. https://doi.org/10.1016/j.carbon.2023.118745.

Mulabagal, V., Liu, L., Qi, J., Wilson, C., Hayworth, J.S., 2018. A rapid UHPLC-MS/MS method for simultaneous quantitation of 23 perfluoroalkyl substances (PFAS) in estuarine water. Talanta 190, 95–102. https://doi.org/10.1016/j.talanta.2018.07.053.

O'Rourke, E., Losada, S., Barber, J.L., Scholey, G., Bain, I., Pereira, M.G., et al., 2024. Persistence of PFOA pollution at a PTFE production site and occurrence of replacement PFASs in English freshwaters revealed by sentinel species, the Eurasian otter (Lutra lutra). Environ. Sci. Technol. 58 (23), 10195–10206. https://doi.org/10.1021/acs.est.3c09405.

Partl, G.J., Naier, B.F.E., Bakry, R., Schlapp-Hackl, I., Kopacka, H., Wurst, K., et al., 2021. Can't touch this: highly omniphobic coatings based on self-textured C6-fluoroponytailed polyvinylimidazolium monoliths. J. Fluor. Chem. 249, 109839. https://doi.org/10.1016/j.jfluchem.2021.109839.

Quan, Q., Wen, H., Han, S., Wang, Z., Shao, Z., Chen, M., 2020. Fluorous-core nanoparticle-embedded hydrogel synthesized via tandem photo-controlled radical polymerization: facilitating the separation of perfluorinated alkyl substances from water. ACS Appl. Mater. Interfaces 12 (21), 24319–24327. https://doi.org/10.1021/acsami.0c04646.

Rahman, M.F., Peldszus, S., Anderson, W.B., 2014. Behaviour and fate of perfluoroalkyl and polyfluoroalkyl substances (PFASs) in drinking water treatment: a review. Water Res. 50, 318–340. https://doi.org/10.1016/j.watres.2013.10.045.

Singh, A., Lynch, R., Solomon, J., Weaver, J.D., May, A.R., 2023. Development of novel fluor mop materials for remediation of perfluoroalkyl substances (PFAS) from groundwater. J. Hazard. Mater. 448, 130853. https://doi.org/10.1016/j.jhazmat.2023.130853.

Tan, X., Dewapriya, P., Prasad, P., Chang, Y., Huang, X., Wang, Y., et al., 2022a. Efficient removal of perfluorinated chemicals from contaminated water sources using magnetic fluorinated polymer sorbents. Angew. Chem. Int. Ed. 61 (49), e202213071. https://doi.org/10.1002/anie.202213071.

Tan, X., Sawczyk, M., Chang, Y., Wang, Y., Usman, A., Fu, C., et al., 2022b. Revealing the molecular-level interactions between cationic fluorinated polymer sorbents and the major PFAS pollutant PFOA. Macromolecules 55 (3), 1077–1087. https://doi.org/10.1021/acs.macromol.1c02435.

Tasfaout, A., Ibrahim, F., Morrin, A., Brisset, H., Sorrentino, I., Nanteuil, C., et al., 2023. Molecularly imprinted polymers for per- and polyfluoroalkyl substances enrichment and detection. Talanta 258, 124434. https://doi.org/10.1016/j.talanta.2023.124434.

Teymoorian, T., Munoz, G., Vo Duy, S., Liu, J., Sauvé, S., 2023. Tracking PFAS in drinking water: a review of analytical methods and worldwide occurrence trends in tap water and bottled water. ACS ES&T Water 3 (2), 246–261. https://doi.org/10.1021/acsestwater.2c00387.

Thomas, H.C., 1944. Heterogeneous ion exchange in a flowing system. J. Am. Chem. Soc. 66 (10), 1664–1666. https://doi.org/10.1021/ja01238a017.

Wang, W., Xu, Z., Zhang, X., Wimmer, A., Shi, E., Qin, Y., et al., 2018. Rapid and efficient removal of organic micropollutants from environmental water using a magnetic nanoparticles-attached fluorographene-based sorbent. Chem. Eng. J. 343, 61–68. https://doi.org/10.1016/j.cej.2018.02.101.

Woodard, S., Berry, J., Newman, B., 2017. Ion exchange resin for PFAS removal and pilot test comparison to GAC. Remediat. J. 27 (3), 19–27. https://doi.org/10.1002/rem.21515.

Woodard, S., Nickelsen, M.G., Sinnett, M.M., 2018. Ion exchange for PFAS removal. In: Kempisty, D.M., Xing, Y., Racz, L. (Eds.), Perfluoroalkyl Substances in the Environment. CRC Press, Boca Raton, pp. 325–352.

Zhang, D.Q., Zhang, W.L., Liang, Y.N., 2019. Adsorption of perfluoroalkyl and polyfluoroalkyl substances (PFASs) from aqueous solution–a review. Sci. Total Environ. 694, 133606. https://doi.org/10.1016/j.eti.2020.100879.